Magn Reson Mater Phy (2006) 19: 297–304
DOI 10.1007/s10334-006-0057-8

RESEARCH ARTICLE

Richard Winkelmann
Peter Börnert
Jan De Becker
Romhild Hoogeveen
Peter Mazurkewitz
Olaf Dössel

Dual-contrast single breath-hold 3D abdominal MR imaging

Received: 24 July 2006
Revised: 20 October 2006
Accepted: 23 October 2006
Published online: 24 November 2006
© ESMRMB 2006

R. Winkelmann (✉) · O. Dössel
Institute of Biomedical Engineering,
University of Karlsruhe, 76128 Karlsruhe,
Germany
E-mail:
Richard.Winkelmann@ibt.uni-karlsruhe.de
Tel.: +49-40-50782494
Fax.: +49-40-50782510

P. Börnert · P. Mazurkewitz
Philips Research Europe - Hamburg,
Roentgenstr. 24–26, 22335 Hamburg,
Germany

J. de Becker · R. Hoogeveen
Philips Medical Systems, Best,
The Netherlands

Abstract *Object:* Multiple contrasts are often helpful for a comprehensive diagnosis. In 3D abdominal MRI, breath-hold techniques are preferred for single contrast acquisitions to avoid respiratory artifacts. In this paper, highly accelerated parallel MRI is used to acquire large 3D abdominal volumes with two different contrasts within a single breath-hold.
Material and methods: In vivo studies have been performed on six healthy volunteers, combining T_1- and T_2-weighted, gradient- or spin-echo based scans, as well as water/fat resolved imaging in a single breath-hold. These 3D scans were acquired with an acceleration factor of six, using a prototype 32-element receive array.
Results: The presented approach was tested successfully on all volunteers. The whole liver area was covered by a FOV of $350 \times 250 \times 200\,mm^3$ for all scans with reasonable spatial resolution. Arbitrary scan protocols generating different contrasts have been shown to be combinable in this single breath-hold approach. Good spatial correspondence with negligible spatial offset was achieved for all different scan combinations acquired in overall breath-hold times between 15 and 25 s.
Conclusion: Enabled by highly parallel imaging technology, this study demonstrates the technical feasibility and the promising image quality of single breath-hold dual contrast MRI.

Keywords Parallel imaging · Multi-contrast · Abdomen · 3D · Breath-hold · Water-fat

Introduction

In abdominal magnetic resonance imaging (MRI), breath-hold techniques are frequently used to avoid image artifacts. Thus, respiratory motion (e.g., of liver and kidneys) is frozen, and also peristaltic motion artifacts can be reduced due to the short total scan duration. However, for a comprehensive diagnosis, large volume coverage (3D) and multiple contrasts, as obtained via T_1-, T_2-weighted or fat-suppressed protocols, are often mandatory [1,2]. Even if parallel imaging [3–5] is used for scan acceleration, on the currently available magnetic resonance (MR) hardware, such multi-contrast examinations require several breath-holds. This increases the risk of spatial misregistration between the individual scans caused by the often limited breath-hold reproducibility in patients [6].

However, MR scanners became recently available, which support a very large number of receive channels [7–9]. In combination with appropriate reception coil arrays, such systems enable highly accelerated parallel imaging, allowing for a considerable shortening of the scanning time or an increase of spatial resolution. This technology offers the opportunity to acquire large abdominal 3D volumes at reasonable spatial resolution within a breath-hold, and, even further, multiple 3D volumes can be acquired during breath-holding. Thus, two or more different image contrasts could be obtained by

combining appropriate MR protocols (regardless if spin-echo or gradient-echo based) within a single breath-hold, which is the core idea of the present paper. Multi-contrast data acquired in this way exhibit almost no spatial mismatch. Thus, without the need of registration, their multi-contrast information, available for each acquired voxel, can either be provided to the user directly for a more comprehensive diagnosis, or can support computer-aided diagnosis (CAD). Recently, the interest in CAD increased [10], mainly driven by the increasing amount of data to be analyzed. Algorithms may pre-select potential areas of interest, reformat typical oblique views or combine data sets in an intelligent way [11,12] to support clinical decision making. All these steps require automatic data analysis, which can significantly benefit from voxel-based multi-contrast information.

This paper demonstrates the practical feasibility of multi-contrast single-breath-hold acquisitions in an in vivo study on healthy volunteers, using highly accelerated parallel imaging techniques like SENSE [4,13]. An appropriate separation and cascading of the individual scan acquisition blocks was performed for an efficient use of the breath-hold period. Based on the promising image quality for the almost simultaneously acquired T_1/T_2 weighted or water/fat resolved data, results are discussed, and potential benefits and applications are outlined.

Methods

Hardware setup and scan orientation

Experiments were performed on a 1.5-T clinical scanner (ACHIEVA, Philips Medical Systems, Best, NL) further expanded with 32 independent receive channels. Radio frequency (RF) transmission was performed using the B_1 homogenous RF body coil, while an experimental 32-element coil was employed for signal reception.

This coil exhibits sufficient spatial coverage, making it applicable for 3D abdominal imaging, too. The coil consists of two independent parts, an anterior and a posterior one, each composed of 16 hexagonal receive coil elements, which are arranged in three rows in feet-head (FH) direction, as shown in Fig. 1. The anterior coil is flexible and can be bent around the patient for an optimal coverage. The posterior part has a pre-bent structure in LR direction and is placed on the patient table.

Using this coil setup, different scan orientations and SENSE reduction factors (R) have been tested. The objective for an optimal setting was to acquire a given non-angulated volume (cf. Fig. 1) with a field of view (FOV) of 350 mm in RL, 250 mm in AP (anterior–posterior) and 200 mm in FH with a resolution of about $2 \times 2 \times 2\,mm^3$ in a minimum time with an optimal signal-to-noise ratio (SNR). Geometry factor considerations, based on the applied reduction factors for the corresponding phase encoding directions, allowed one to compare the SNR-loss for the different settings. In practice, the reduction factors are roughly limited by the number of diversifying elements in the corresponding direction, which will be named coil factor in the following. The used coil array had a coil factor of five in LR, two in AP and three in FH direction. Aiming for the maximum reduction factor, one would suggest to choose the readout direction in AP, and phase encoding in FH and LR, taking advantage of the high coil diversity in LR. However, in this case, not only the torso, but also all body parts including the arms have to be encoded to prevent folding artifacts requiring a large FOV (up to 500 mm) in this direction. Furthermore, as confirmed by own simulations, not shown here, an acceleration factor R_{LR} of 5 leads to high g-factors for this particular coil, especially in the inner body region which is already low in SNR. This corresponds to Wiesinger's findings, that high reduction factors can be problematic [14]. It is important to note that there are different settings of phase encoding directions and corresponding reduction factors feasible for the same total measuring time. Among them, the one was chosen for the present study in which the phase encoding directions were aligned to smallest FOV dimensions. This allowed the application of the lowest SENSE reduction factors to minimize the noise amplification described by the g-factor [4,13].

In consequence, phase encoding was applied in AP and FH, and readout was performed in LR to take advantage of the signal suppressing ability of the anti-aliasing filters present in the readout channel. Slice selection was applied in the FH direction, employing a slight oversampling to compensate for the finite quality of the slice profile. The reduction factors were chosen according to the coil factors with $R_{AP} = 2$ and $R_{FH} = 3$, resulting in an overall acceleration factor of 6. This reflects a good compromise between noise propagation on the one hand and scanning time on the other hand for this coil array.

Coil sensitivity reference data were obtained in a low-resolution 3D volume scan (voxel size $11 \times 15 \times 15\,mm^3$). This resolution was found to be sufficient to cover the main sensitivity features of the employed 32-element coil. During free breathing, coil array data and body coil data were acquired in an interleaved way within 30 s total scan time. Data processing [4] subsequently performed yielded the coil sensitivity maps.

Preparation phase and actual scan separation

The use of the 32-element coil in combination with SENSE acceleration allows a significant scan time reduction. Depending on the actual scan protocol, data acquisition takes about 5–15 s. However, this is only correct for the net scan time, excluding the scan preparation phase. On the MR system used in this study, such a preparation phase is used to optimize certain general scan parameters like the Larmor frequency, shim settings or transmit gain. However, there are other parameters like receiver gain, trims for turbo spin echo (TSE) scans or echo-planar imaging (EPI) phase corrections that have to be specifically tailored to the individual scan and consequently differ from protocol to protocol. The preparation phase is usually performed directly before each scan, and hence does not affect a standard scanning procedure (see Fig. 2a). However, if two different scans should be combined within one breath-hold, the second scan preparation phase has to be executed directly before the real data acquisition of the second scan. This spoils the scan efficiency during the breath-hold, which

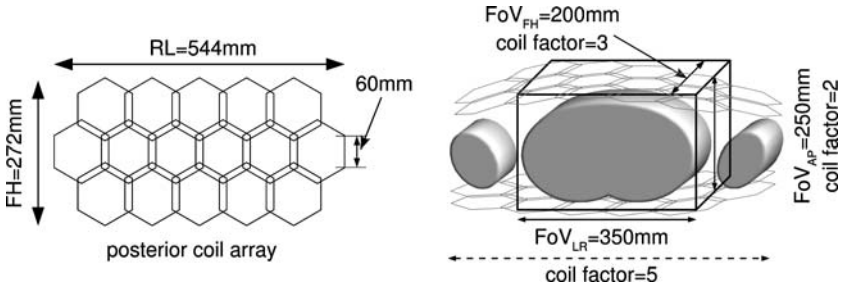

Fig. 1 Coil array setup and FOV definition. The posterior array consists of 16 hexagonal elements, which are grouped in three rows in FH-direction as shown on the left. The flexible anterior array exhibits a nearly similar arrangement. The FOV definition used in this study is shown on the right. The 3D-volume was acquired with a SENSE factor of three in FH and two in AP direction, according to the corresponding coil factors. Read-out and slab selection were performed in LR and FH, respectively

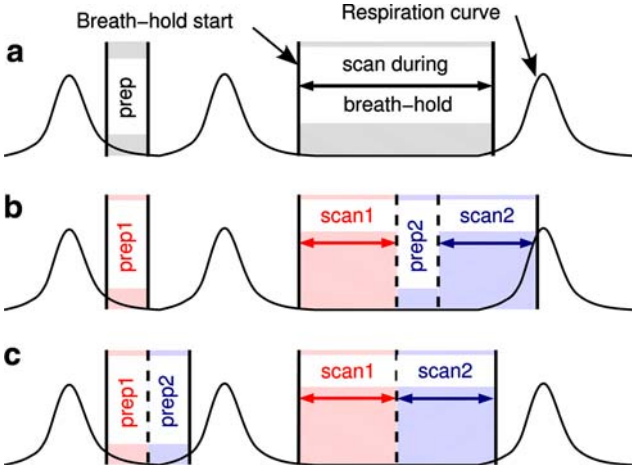

Fig. 2 Preparation phase separation. Standard breath-hold techniques perform the scan preparation phase separately but just before the scan **(a)**. The acquisition of multiple scans with different contrasts within a breath-hold results in timing conflicts due to the preceding preparation for scan two **(b)**. This can be avoided, if the preparation phases and the actual data acquisition are separated and appropriately grouped as shown in **c**

is illustrated in Fig. 2b. However, by separating the preparation phases of each scan and appropriate grouping, they can be performed beforehand, either during free breathing or in a preceding breath-hold (Fig. 2c). Defining and grouping the protocols this way allowed the actual data sampling for the two scans with a delay of only about one second.

Selected contrast protocols for scan combination

Combinations of different contrast protocols have been performed on six healthy volunteers (all male, 28–37 years) with informed consent obtained. Mostly T_1- and T_2-weighted scans have been combined, optimized for a 3D acquisition to cover the entire liver. Two different T_1-weighted sequences have been used in this study, a magnetization-prepared (using a fat suppression RF pre-pulse), segmented T_1-weighted gradient echo sequence (called THRIVE in the following) and a conventional T_1-weighted fast gradient echo sequence (FFE), acquired with Half Fourier encoding [15].

These were combined with either a T_2/T_1-weighted balanced steady state free precession sequence (BFFE), or with a mainly T_2-weighted TSE sequence. The TSE sequence was acquired using Half Fourier and a driven equilibrium Fourier transform approach [16] that flips back the transverse magnetization to M_Z at the end of the echo train to allow for shortening the repetition time.

Table 1 summarizes the different scan combinations used in this study, including their most relevant parameters. All scans have been acquired during breath holding in the end-expiratory phase, considering an overall breath-hold of about 20 s as acceptable.

A color-coding overlay has been used as a simple post-processing to visualize the spatial correspondence of the two individual data sets acquired in the same breath-hold. Thus, an orange color map was applied to the T_1-weighted scans, while a blue map was used for the T_2 (or T_2/T_1) - weighted ones.

Water and fat acquisition schemes

To follow the concept to acquire multiple contrasts in a single breath-hold, water/fat imaging can be considered too. Two different approaches have been used in this work. First a magnetization-prepared segmented gradient echo approach (w/f-TFE) that either suppresses the water or the fat signal was used. Both scans, the water and the fat selective one, can be performed subsequently in a single breath-hold. The actual sequence is rather similar to the THRIVE sequence described above. The corresponding scan parameters chosen for this single breath-hold water/fat approach are given in the protocol D in Table 1.

Another approach for water/fat resolved imaging is a chemical shift encoding technique that uses multiple gradient echoes sampled at different echo times. In the present work, three gradient echoes were acquired at different echo times to allow the fitting of water and fat signals and the local off-resonance

Table 1 Scan combination protocols A–E

Scan parameters for selected contrast combinations					
Comb	Res (mm^3)		Seq	TR/TE/FA	T_{scan}(s)
A	2.2^3	T1	FFE	4.0 ms/1.9 ms/10°	5.4 s
		T2	TSE	307 ms/70 ms/90°	14.7 s
B	1.4×1.4×3	T1	FFE	4.3 ms/2.1 ms/10°	6.4 s
		T2	BFFE	3.3 ms/1.6 ms/50°	8.2 s
C	2.2^3	T1	THRIVE	4.3 ms/2.0 ms/10°	13.1 s
		T2	BFFE	3.0 ms/1.5 ms/50°	5.4 s
D	2.0 × 2.0 × 3	w	w-TFE	4.4 ms/2.1 ms/10°	11.8 s
		f	f-TFE	4.4 ms/2.1 ms/10°	11.8 s
E	2.0 × 2.0 × 3	w + f	ME-FFE	9.5 ms/2.0 + 4.4 + 6.8 ms/15°	20.4 s

Each protocol comprises two different scans (exception E) with different contrasts (T1, T2, water, fat) performed in a single breath-hold to cover a 3D volume as shown in Figure 2. Basic parameters are summarized (voxel size, repetition time, echo time, flip angle and scan duration)

additionally [17]. Three echoes can be acquired in three separate scans, grouped together into a breath-hold, which, however, is not very efficient. Thus, a multi-echo readout was chosen to acquire three echoes after one excitation in a FFE sequence similar to an approach recently suggested [18]. To avoid eddy-current related artifacts, a fly back echo-planar [19] like acquisition was performed to sample the echoes at the same readout gradient polarity. This is basically a single scan performed in a single breath-hold, but the sequence delivers three 3D data sets at different TEs. The corresponding scan parameters are given under the protocol E in Table 1.

Results

Different combinations of the previously described individual sequences (protocol A–E) have successfully been tested in vivo. Figure 3 shows selected slices of the two different 3D data sets, acquired according to protocol A in a total breath-hold of 21 s. Reformatting for different scan orientations is shown for these isotropic data.

Figure 4 shows results measured with protocol B in another volunteer, acquired in a total breath-hold time of about 16 s. The lower intrinsic SNR of the T_1-weighted sequence is visible, especially in the central region (Fig. 4a), where a maximum noise amplification of the SENSE algorithm occurs. The color-coded overlay of the two scans, given in Fig. 4c, demonstrates the good spatial correspondence.

Results of the protocol C, obtained in a total breath-hold of less than 20 s, are shown in Fig. 5. Selected slices of the two different isotropic 3D data sets are shown. Additionally, the color-overlay of the two scans, reformatted to all basic scan orientations, is shown to underline the good spatial consistency (Fig. 5c).

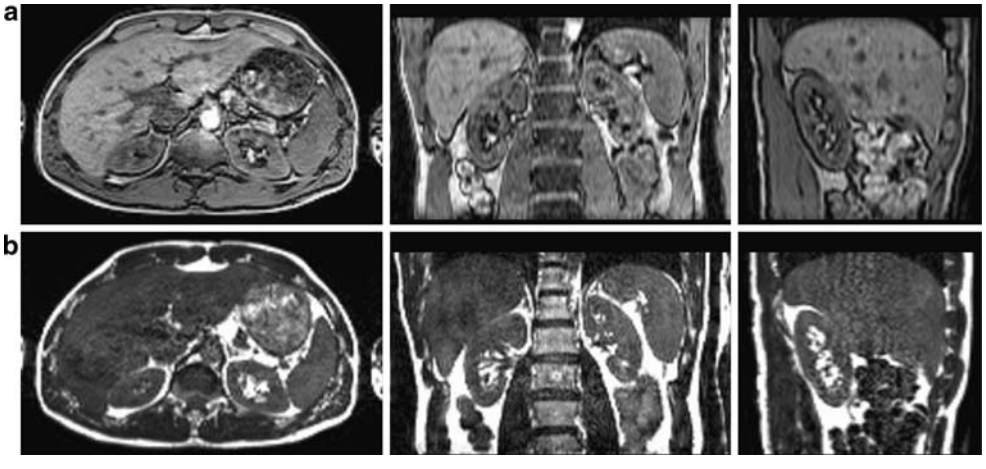

Fig. 3 Combined dual contrast 3D-FFE/TSE (protocol A). A T_1-FFE was acquired together with a TSE sequence in a single breath-hold. Selected reformatted slices acquired with the T_1-weighted sequence are shown in **a**, while the corresponding T_2-weighted TSE slices are given in **b**

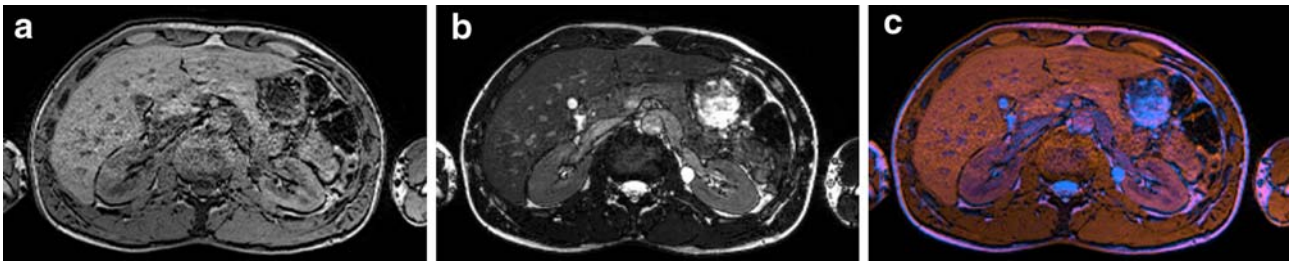

Fig. 4 Combined dual contrast 3D-FFE/BFFE (protocol B). The abdominal volume was acquired with a T_1-FFE **(a)** and a T_2/T_1-weighted BFFE sequence **(b)** using a non-isotropic resolution. The color-overlay of the two scans, acquired within the same breath-hold, is given in **c**

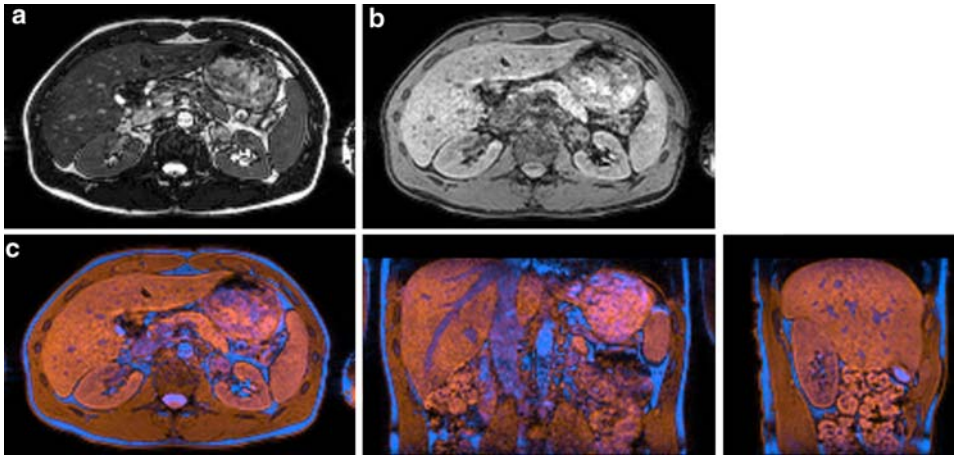

Fig. 5 Combined dual contrast 3D-BFFE/THRIVE (protocol C). A balanced FFE sequence **(a)** was combined with a fat-suppressed THRIVE sequence **(b)** in a single breath-hold. Color-overlays of the two scans are shown in **c** and two reformatted slices are shown additionally (transversal, coronal, sagittal)

Results from the two different water/fat separation schemes, investigated in this study, are compared. Figure 6a,b shows a slice of the 3D fat- and water-suppressed data, acquired in a single breath-hold of 25 s. These data are compared to results of a three-echo chemical shift encoded scan of the same slice in the same volunteer (Fig. 6c, d). This scan was slightly more time-efficient and allowed a total scan time of 20 s. The arrow in Fig. 6a indicates a region with local field inhomogeneity showing a limitation of the magnetization preparation in case of strong susceptibility gradients. The chemical shift encoding approach performed more robust in this respect and showed furthermore a better SNR (Fig. 6c).

Discussion

The basic feasibility to acquire two 3D data sets with different contrasts within a single breath-hold has been shown successfully. Thus, different contrast combinations of T_1- and T_2-weighted, or water/fat resolved 3D data sets can be acquired in a single breath-hold with reasonable spatial resolution and coverage.

The protocols used in this study are standard protocols available on every modern MRI scanner. No specific sequence tuning was necessary and arbitrary scan combinations are possible. However, all scans were acquired in the 3D-mode to benefit from the SNR gain due to the averaging effect and the full parallel imaging performance in slice direction [13]. While the basic feasibility was demonstrated, further efforts are necessary to improve the image quality for routine clinical use. This is especially true for the TSE example given in Fig. 3, which shows a limited SNR due to the time constraints for T_1 relaxation. However, TSE could potentially be replaced by balanced BFFE in abdominal imaging as recently discussed in Ref. [20]. The order of the protocol combinations does not underlie any serious restrictions. However, a minimum time delay between the scans is desirable for T_1 relaxation. Thus, low flip angle gradient echo sequences were preformed first, where the magnetization returns faster to the equilibrium after the scan, compared to TSE or BFFE sequences with their intrinsic high flip angles. In this study, a scan delay of about one second was used, which seems to be a reasonable compromise.

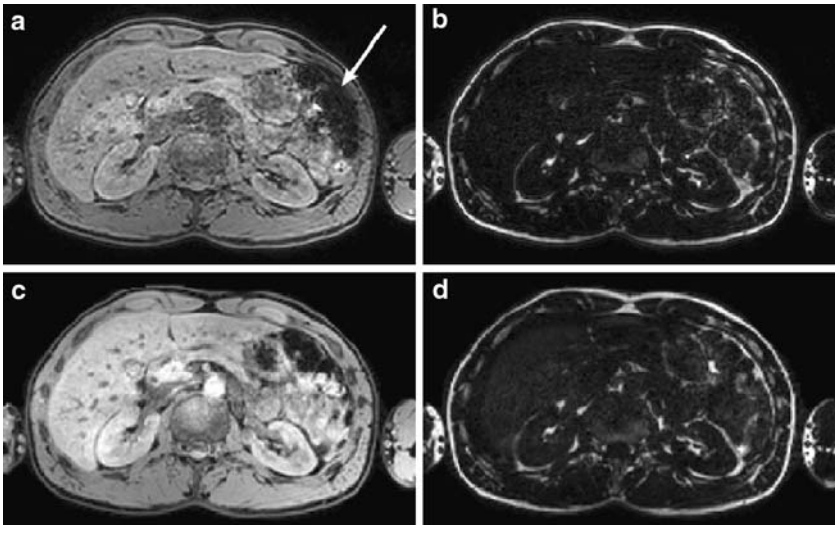

Fig. 6 Comparison of two different simultaneous 3D water/fat acquisition approaches. Images obtained by the combined dual contrast water- or fat- suppression (protocol D) and three-point chemical shift encoding ones (protocol E) are shown in **a, b** and **c, d**, respectively. Fat-suppression was applied in **a**, which also suppressed water signal near the tissue-air interfaces due to insufficient shim (arrow). Fat-only data have been generated by water-suppression **(b)**. Both 3D data sets were acquired in a single breath-hold. The lower two images were reconstructed from a 3D three-echo acquisition, employing an iterative reconstruction to separate water **(c)** and lipid signal **(d)**

Water/fat resolved imaging is important for a number of applications, for instance for the diagnosis of obesity [21]. As demonstrated in Fig. 6a, b, magnetization prepared approaches can be used for single breath-hold water and fat imaging. However, this approach can show artifacts in the presence of spatial off-resonance, as it is demonstrated in Fig. 6a. This can be overcome using three-echo chemical shift encoding, which is able to cope with the off-resonance problem [17]. Its better performance compared to the magnetization prepared approach is visible in Fig. 6. Furthermore, due to the intrinsic signal averaging effect of the three-echo approach [22], the SNR in the water/fat data is much better than for the chemical shift selective approach. Also with respect to scan efficiency, the specific multi-echo approach chosen in this work has shown a better performance resulting in a shorter total breath-hold for the same spatial resolution and volume coverage.

In this study, isotropic and non-isotropic scan resolutions have been presented. In case of subsequent data reformatting to different orientations and angulations, isotropic scan resolution seems to be preferable; otherwise, a non-isotropic resolution may represent a more efficient alternative.

Significantly higher spatial resolution, albeit desirable, may be difficult to realize. A higher scan acceleration with moderate g-factors using specifically optimized receive arrays might be feasible. However, a high SNR gain due to significantly lower g-factors should not be expected, as the mean g-factor for the actual coil array already remained below 1.1 (with maximum values around 1.5). Furthermore, the intrinsic available SNR is proportional to the voxel size and the square root of the scan time. Because of the single breath-hold approach, small voxel sizes cannot be compensated by long scan times. Hence, this clearly indicates limitations of the scan resolution due to SNR restrictions.

Furthermore, possible organ drifts during the breath-hold itself limit the scan resolution in practice [23]. A retrospective registration and motion correction can help to correct for such drifts between two data sets acquired within a single breath-hold. However, in cases where contrast differs a lot, registration can become rather difficult and time consuming [24], and non-deterministic motion like peristaltic motion can even complicate this task. In the presented approach, the latter problem is reduced due to the very short time delay between the scans. Nevertheless, if higher spatial resolution is required, free-breathing techniques using navigators [25] or self-navigation approaches [26,27] seem to hold higher potential.

The coil used in this study was not designed for abdominal imaging. Its FH-coverage is rather limited. A different coil arrangement, e.g., consisting of four element rows in FH, would allow a higher spatial coverage and a higher SENSE factor in this direction. This means that the higher coverage, if allowed by the coil geometry, can be achieved keeping scan time and resolution constant. The SENSE factor in AP, however, seems to be limited to a factor of two. Nevertheless, further investigations are needed to give a final answer.

The multi-contrast 3D data sets can be analyzed directly on a voxel-by-voxel basis without any post-processing steps, as shown for example in the color-overlays

of Fig. 4 and Fig. 5. However, the added value of the color-overlay is limited. The intelligent use of this voxel-based multi-contrast information is still an open question, which might be answered in further research dedicated to computer-aided diagnosis (CAD).

Conclusion

The acquisition of a large 3D volume with separate scans of different contrasts, but within one breath-hold, is demonstrated in this work. The new capabilities of parallel imaging allowed a diagnostically relevant spatial resolution and volume coverage. Data sets without spatial misregistration were obtained, which can be further processed without any registration to support computer-aided diagnosis. Especially for diagnoses that use breath-hold techniques and that are based on multiple contrasts, the presented approach may enable a more comfortable and accurate diagnosis and may help to improve clinical workflow.

Acknowledgments The authors would like to thank Holger Eggers (Philips Research Europe–Hamburg) for software support.

References

1. Semelka RC, Martin DR, Balci C, Lance T (2001) Focal liver lesions: comparison of dual-phase CT and multisequence multiplanar MR imaging including dynamic gadolinium enhancement. J Magn Reson Imaging 13:397–401
2. Klessen C, Asbach P, Kroencke TJ, Fischer T, Warmuth C, Stemmer A, Hamm B, Taupitz M (2005) Magnetic resonance imaging of the upper abdomen using a free-breathing T2-weighted turbo spin echo sequence with navigator triggered prospective acquisition correction. J Magn Reson Imaging 21:576–582
3. Sodickson DK, Manning WJ (1997) Simultaneous acquisition of spatial harmonics (SMASH): fast imaging with radiofrequency coil arrays. Magn Reson Med 38:591–603
4. Pruessmann KP, Weiger M, Scheidegger MB, Boesiger P (1999) SENSE: sensitivity encoding for fast MRI. Magn Reson Med 42:952–962
5. Griswold MA, Jakob PM, Heidemann RM, Nittka M, Jellus V, Wang J, Kiefer B, Haase A (2002) Generalized autocalibrating partially parallel acquisitions (GRAPPA). Magn Reson Med 47:1202–1210
6. Liu YL, Riederer SJ, Rossman PJ, Grimm RC, Debbins JP, Ehman RL (1993) A monitoring, feedback, and triggering system for reproducible breath-hold MR imaging. Magn Reson Med 30:507–511
7. Zhu Y, Hardy CJ, Sodickson DK, Giaquinto RO, Dumoulin CL, Kenwood G, Niendorf T, Lejay H, McKenzie CA, Ohliger MA, Rofsky NM (2004) Highly parallel volumetric imaging with a 32-element RF coil array. Magn Reson Med 52:869–877
8. Wintersperger BJ, Reeder SB, Nikolaou K, Dietrich O, Huber A, Greiser A, Lanz T, Reiser MF, Schoenberg SO (2006) Cardiac CINE MR imaging with a 32-channel cardiac coil and parallel imaging: impact of acceleration factors on image quality and volumetric accuracy. J Magn Reson Imaging 23:222–227
9. Nehrke K, Börnert P, Mazurkewitz P, Winkelmann R, Graesslin I (2006) Free-breathing whole-heart coronary MR angiography on a clinical scanner in four minutes. J Magn Reson Imaging 23:752–756
10. Doi K (2005) Current status and future potential of computer-aided diagnosis in medical imaging. Br J Radiol 78:S3-S19
11. Danilouchkine MG, Westenberg JJ, van Assen HC, van Reiber JH, Lelieveldt BP (2005) 3D model-based approach to lung registration and prediction of respiratory cardiac motion. Med Image Comput Comput Assist Interv Int Conf Med Image Comput Comput Assist Interv 8:951–959
12. Noble NM, Muthurangu V, Boubertakh R, Winkelmann R, Johnson RA, Hedge S, Börnert P, Razavi RS, Hill DL (2006) 32-Channel non-angulated cine cardiac volumes—automatic reformatting. In: Proceedings of 14th scientific annual meeting, Seattle, p. 791
13. Weiger M, Pruessmann KP, Boesiger P (2002) 2D SENSE for faster 3D MRI. Magn Reson Mater Phy 14:10–19
14. Wiesinger F, Boesiger P, Pruessmann KP (2004) Electrodynamics and ultimate SNR in parallel MR imaging.Magn Reson Med 52:376–390
15. Feinberg DA, Hale JD, Watts JC, Kaufman L, Mark A (1986) Halving MR imaging time by conjugation: demonstration at 3.5 kG. Radiology 161:527–531
16. Hargreaves BA, Gold GE, Lang PK, Conolly SM, Pauly JM, Bergman G, Vandevenne J, Nishimura DG (1999) MR imaging of articular cartilage using driven equilibrium. Magn Reson Med 42:695–703
17. Reeder SB, Wen Z, Yu H, Pineda AR, Gold GE, Markl M, Pelc NJ (2004) Multicoil Dixon chemical species separation with an iterative least-squares estimation method. Magn Reson Med 51:35–45
18. Shankaranarayanan A, Sodickson D, Giaquinto R, Grant A, Carrillo A, Gurr D, Madhuranthakam A, Yu H, Shimakawa A, Joshi S, Dumoulin C, Reeder S, Steger T, Brau A, Farrar N, Rofsky N, LaRuche S, Brittain J, McKenzie C (2006) Highly accelerated IDEAL for volumetric abdominal imaging with fat-water separation in a single breath-hold. In: Proceedings of the 14th scientific annual meeting, Seattle, p. 2453
19. Feinberg DA, Turner R, Jakab PD, von Kienlin M (1990) Echo-planar imaging with asymmetric gradient modulation and inner-volume excitation. Magn Reson Med 13:162–169
20. Herborn CU, Vogt F, Lauenstein TC, Goyen M, Debatin JF, Ruehm SG (2003) MRI of the liver: can True FISP replace HASTE? J Magn Reson Imaging 17:190–196
21. Kovanlikaya A, Mittelman SD, Ward A, Geffner ME, Dorey F, Gilsanz V (2005) Obesity and fat quantification in lean tissues using three-point Dixon MR imaging. Pediatr Radiol 35:601–607

22. Pineda AR, Reeder SB, Wen Z, Pelc NJ (2005) Cramer-Rao bounds for three-point decomposition of water and fat. Magn Reson Med. 54:625–635.
23. Taylor AM, Jhooti P, Keegan J, Simonds AK, Pennell DJ (1999) Magnetic resonance navigator echo diaphragm monitoring in patients with suspected diaphragm paralysis. J Magn Reson Imaging 9:69–74
24. Fischl B, Salat DH, van der Kouwe AJ, Makris N, Segonne F, Quinn BT, Dale AM (2004) Sequence-independent segmentation of magnetic resonance images. Neuroimage 2:69–84
25. Sachs TS, Meyer CH, Hu BS, Kohli J, Nishimura DG, Macovski A (1994) Real-time motion detection in spiral MRI using navigators. Magn Reson Med 32:639–645
26. Schaeffter T, Rasche V, Carlsen IC (1999) Motion compensated projection reconstruction. Magn Reson Med 41:954–963
27. Stehning C, Börnert P, Nehrke K, Eggers H, Stuber M (2005) Free-breathing whole-heart coronary MRA with 3D radial SSFP and self-navigated image reconstruction. Magn Reson Med 54:476–480